FACULDADE DE MEDICINA DA UNIVERSIDADE DE COIMBRA

TRABALHO FINAL DO 6º ANO MÉDICO COM VISTA À ATRIBUIÇÃO DO GRAU DE MESTRE NO ÂMBITO DO CICLO DE ESTUDOS DE MESTRADO INTEGRADO EM MEDICINA

JOÃO PEDRO DOS SANTOS FILIPE

DIFFUSION-WEIGHTED IMAGING OF THE LIVER: VALUE OF APPARENT DIFFUSION COEFFICIENT AND INFLUENCE OF REGION OF INTEREST

ARTIGO CIENTÍFICO

ÁREA CIENTÍFICA DE IMAGIOLOGIA

TRABALHO REALIZADO SOB A ORIENTAÇÃO DE:
PROFESSOR DOUTOR FILIPE CASEIRO ALVES
DR. LUIS CURVO SEMEDO

04/2011

The following manuscript was written according to the **"Uniform Requirements for Manuscripts Submitted to Biomedical Journals: Writing and Editing for Biomedical Publication"**, April 2010 update, published by the International Committee of Medical Journal Editors and free accessible at *http://www.icmje.org.*

Diffusion-weighted Imaging of the Liver: value of apparent diffusion coefficient and influence of region of interest

João Filipe, Luís Semedo, Filipe Caseiro-Alves

Faculdade de Medicina, Universidade de Coimbra, Portugal

Clínica Universitária de Radiologia, Hospitais da Universidade de Coimbra, Portugal

Contact information:

João Pedro dos Santos Filipe; address: Beco das Palheiras, nº 7, 2430-605 Vieira de Leiria, Portugal; telephone number: +351 917134410; e-mail address: mail.jpfilipe@gmail.com.

Number of Figures: 7; N**umber of Tables:** 3

LIST OF ABBREVIATIONS

DWI = Diffusion-Weighted Imaging

MR = Magnetic Resonance

ADC = Apparent Diffusion Coefficient

ROI = Region of Interest

EPI = Echo-planar Imaging

RT = Respiratory Triggering

SNR = Signal-to-noise Ratio

SD = Standard Deviation

HCC = Hepatocellular Carcinoma

FNH = Focal Nodular Hyperplasia

ABSTRACT

Purpose: To measure apparent diffusion coefficient (ADC) values of liver parenchyma and focal hepatic lesions (FHL), investigate the utility of ADC for the differential diagnosis of hepatic findings, and determine the influence of region of interest (ROI) characteristics in the overall ADC measurements.

Materials and Methods: Ninety-three patients (47 men, 46 women; mean age, 58 years) with at least one FHL ≥ 10 mm, or parenchyma abnormalities, were retrospectively evaluated. Reference standard for diagnosis was obtained from histopathologic data, consensus between imaging methods, follow-up imaging and patient clinical history. A total of 90 lesions were evaluated: 14 hepatocellular carcinomas (HCC), 18 metastases, 10 focal nodular hyperplasias (FNH), 4 adenomas, 30 hemangiomas and 14 cysts. Respiratory-Triggered (RT) DWI was performed using b-values of 50 and 700 s/mm^2. ADC was measured in hepatic parenchyma by placing ROIs in four different segments, and in FHL by using three circular 1 cm^2 ROIs and one ROI encompassing all lesion volume. Data was statistically compared in SPSS software using the Mann-Whitney and Friedman tests. Wilcoxon test was used to confirm ROI influence and receiver operating characteristic (ROC) curve was analyzed to evaluate the utility of ADC for diagnosis of malignancy. $P<0.05$ was significant.

Results: Mean ADCs ($\times 10^{-3}$mm^2/s) were 1.45, 1.28 and 1.25 for normal, cirrhotic and steatotic liver parenchyma and 1.16, 1.18, 1.30, 1.64, 1.89 and 2.77 for metastases, HCCs, adenomas, FNHs, hemangiomas and cysts, respectively. Parenchyma ADCs in segment II were significantly higher than in any other region. ADCs of malignant lesions were significantly lower than those of benign lesions ($p<0.001$). Individually, ADCs of Cysts were

significantly higher than all other lesions except hemangiomas. There was significant overlap between benign solid lesions and malignant lesions and between HCCs and cirrhotic parenchyma. The area under the curve for diagnosis of malignancy was 0.939, with sensitivity of 89.7% and specificity of 90.6%, using a cutoff ADC of 1.43×10^{-3} mm^2/s. No significant difference was found between the different ROI sampling methods, but only homogeneous lesions were studied.

Conclusion: We concluded that (a) quantitative measurements of ADC can be useful in differentiating normal from pathological liver parenchyma and in the characterization of focal hepatic lesions, (b) left hepatic lobe is more subject to cardiac motion artifacts, and (c) the size of ROI does not influence ADC measurements in homogeneous lesions.

Word Count: 382

Keywords: apparent diffusion coefficient; diffusion weighted imaging; focal hepatic lesions; liver MRI; region of interest

RESUMO

Objectivo: Medir o coeficiente de difusão aparente (ADC) do parênquima hepático e de lesões hepáticas focais (LHF), investigar a utilidade do ADC no diagnóstico diferencial de lesões hepáticas e determinar a influência das características da região de interesse (ROI) nos valores de coeficiente obtidos.

Materiais e Métodos: Noventa e três doentes (47 homens, 46 mulheres; idade média, 58 anos) com pelo menos uma LHF maior ou igual que 10 mm, ou parênquima patológico, foram retrospectivamente avaliados. Confirmação diagnóstica foi obtida por histopatologia, concordância entre métodos de imagem, *follow-up* e historial do doente. No total, 90 lesões foram avaliadas: 14 carcinomas hepatocelulares (CHC), 18 metástases, 10 hiperplasias nodular focais (HNF), 4 adenomas, 30 hemangiomas e 14 quistos. Foi efectuado estudo ponderado em difusão com *trigger* respiratório (valores b de 50 e 700 s/mm^2). Medições de ADC foram efectuadas no parênquima através de ROIs colocadas em quarto segmentos hepáticos e, nas LHF, através de três ROIs de 1 cm^2 e uma ROI englobando toda a lesão. O tratamento estatístico foi efectuado, através do software SPSS, pelos testes Mann-Whitney e Friedman. O teste Wilcoxon foi utilizado para confirmar a influência do ROI e uma curva ROC foi analisada para avaliar o ADC como ferramenta diagnóstica de malignidade. $P<0.05$ foi considerado significativo.

Resultados: ADCs médios ($\times 10^{-3}$mm^2/s) foram 1.45, 1.28 e 1.25 para parênquima normal, cirrótico e esteatótico, e 1.16, 1.18, 1.30, 1.64, 1.89 e 2.77 para metástases, CHCs, adenomas, HNFs, hemangiomas e quistos, respectivamente. ADCs medidos ($\times 10^{-3}$mm^2/s) no parênquima do segmento II foram significativamente mais altos do que em qualquer outro

segmento. Lesões malignas apresentaram ADCs significativamente mais baixos que lesões benignas ($p<0.001$). Individualmente, os ADCs de quistos foram significativamente maiores do que os de outras lesões, exceptuando hemangiomas. Verificou-se uma sobreposição significativa entre lesões sólidas benignas e leso+es malignas, e entre CHCs e parênquima cirrótico. A área sobre a curva para diagnóstico de malignidade foi 0.939, com um ADC limiar de 1.43×10^{-3} mm^2/s (sensibilidade de 89.7% e especificidade de 90.6%). Não foi encontrada diferença significativa entre as medições efectuadas com as ROIs de diferentes tamanhos.

Conclusão: Concluímos que (a) medições quantitativas de ADC são úteis na distinção entre parênquima normal e patológico e na caracterização de LHF, (b) o lobo hepático esquerdo é mais susceptível a artefactos cardíacos, e (c) o tamanho da ROI não influencia o valor do ADC calculado.

Palavras: 387

Palavras-Chave: coeficiente de difusão aparente; difusão; lesões hepáticas focais; ressonância magnética hepática; região de interesse

INTRODUCTION

Diffusion is a physical process that relies on the internal, thermally driven, random motion of water molecules, known as Brownian motion (1-3). Within biologic tissues, the movement of water is not completely random, but rather, is affected by cell organization, density, microstructure, microcirculation and interaction with tissue compartments (1-4). The first diffusion-weighted imaging (DWI) sequence, an adaptation of a T2-weighted sequence, was described by Stejskal and Tanner in 1965 (4). Prior to the development of fast MR techniques, the only successful clinical application was in cranial examinations (3,5) but, with the development of echo-planar imaging techniques, they started being used in abdominal conditions (6,7), especially for the evaluation of organs such as liver, kidney, prostate and rectum (1-3,5).

The sensitivity of a DWI sequence is characterized by its b-value (s/mm^2). When at least two b-values are used, quantitative analysis can be performed by measuring the apparent diffusion coefficient (ADC) of tissues. The automated ADC values for all voxels are usually displayed as a parametric map and regions of interest (ROI) can be drawn within it, providing a non-invasive indirect quantification of cellularity.

DWI may be performed with different techniques like spin-echo (SE), fast spin-echo (FSE), gradient-echo (GE), or echo-planar imaging (EPI) (8,9), and the scanning can be carried out in free breathing, breath-hold or respiratory triggering (RT) (10,11). In clinical practice, respiratory-triggered EPI with fat suppression is the gold-standard DW-MR technique (10). Several publications reported the use of DWI for (a) liver lesion detection and characterization (6,7,10-21), with better results compared with those of T2-weighted imaging (14,16,18); (b) evaluation of diffuse liver disease, which may imply some difficulties with

conventional MR imaging (6,15,20,22-24); (c) predicting the response of malignant tumors to chemotherapy (25,26) and (d) follow-up after chemotherapy (8) or loco-regional therapy (27).

The major limitations of DWI include the low signal-to-noise ratio (SNR), low spacial resolution, and the susceptibility to artifacts (mainly distortion, ghosting, and blurring due to respiratory, cardiac or voluntary movements) associated with EPI (9,10). However, DWI is an attractive technique because (a) it can add qualitative and quantitative information to conventional imaging sequences; (b) it is quick and easy to repeat; (c) it is easily incorporated to existing protocols; (d) it is performed without the use of ionizing radiation or contrast media injection and (e) provides information about tissue cellularity and the integrity of cellular membranes (1-3,8). Nowadays, the clinical impact of hepatic DWI is still under some controversy. The quantitative ADC evaluations are variable and not easily comparable across studies, and the reproducibility, especially when it comes to ROI number, size and position, has not been fully investigated (6,12,13,22,24,28).

Hence, the aim of our study was to (a) obtain quantitative ADC measurements of liver parenchyma and focal hepatic lesions, and determine their contribution to differential diagnosis; (b) determine a threshold ADC value to differentiate benign from malignant lesions and (c) determine the influence of the lesion's ROI size and position in the measured ADC values.

MATERIALS AND METHODS

Study Population

During an 8-month period (August 2009 to April 2010), DW-EPI was performed as part of a routine liver imaging protocol in 194 patients. In 14 patients, no DW images were available for review and in 14 patients, no focal hepatic lesions and/or parenchyma abnormalities were found. Of the remaining 166 patients, 73 were excluded because: (a) motion artifacts were present (n=7), (b) chemotherapy (n=4), thermal ablation (n=6) or metastasectomy (n=4) had been performed, (c) not enough liver parenchyma was available due to right hepatectomy (n=3), left hepatectomy (n=2) or multiple lesions infiltrating all parenchyma (n=10), (d) insufficient data to confirm the nature of the lesions (n=21) and (e) no focal hepatic lesions $\geq$ 10 mm were found (n=16). Therefore, our retrospective analysis included a total of 93 patients (47 men, 46 women, age range: 26-86 years, mean age: 58 years), 12 of which without focal hepatic lesions but with cirrhosis or steatosis, 16 with focal hepatic lesions and cirrhosis or steatosis and 65 with focal hepatic lesions but without parenchyma abnormalities. Different types of lesions were coexisting in 9 patients. In patients with multiple lesions, only the largest lesion was considered and in patients with different types of lesions only the largest lesion of each type was considered. Therefore, a total of 90 focal hepatic lesions were evaluated.

Histopathological characterization of liver parenchyma or focal lesion was the reference standard. When unavailable, a surrogate diagnosis was achieved through a combination of the following criteria: (a) concordance between two or more imaging studies, (b) stability of the lesion within a minimum follow-up of 6 months and (c) clinical history of the patient.

There were 32 malignant tumors (14 hepatocellular carcinomas and 18 metastases). The primary sites of the metastatic lesions included: colorectal carcinoma (n=12), gastric carcinoma (n=2), ovarian carcinoma (n=1), endometrial carcinoma (n=1), renal cell carcinoma (n=1) and neuroendocrine carcinoma (n= 1). Of the 58 benign lesions, 14 were hepatocellular lesions (10 focal nodular hyperplasias and 4 adenomas) while 44 were of non-hepatocellular nature (30 hemangiomas and 14 cysts).

MR Imaging

MR imaging was performed on a 1.5-T system (Symphony Class, Siemens, Erlangen, Germany). The routine MRI protocol included a breath-hold T1-weighted study with in-phase and out-of-phase sequences (TR, 100 ms; TE, 2.32/5.24 ms; flip angle, 70°; matrix, 256 × 180; slice thickness, 9 mm; intersection gap, 1,8 mm; field of view, 350 × 350 mm) and a respiratory-triggered T2-weighted FSE sequence (TR/TE, 1800/93 ms; flip angle, 150°; fat suppression, matrix, 384 × 264; slice thickness, 8 mm; intersection gap, 1,6 mm; field of view, 360 × 270 mm). A dynamic contrast-enhanced 3D gradient-echo volumetric interpolated breath-hold examination sequence was performed before and after contrast enhancement, in the arterial, portal venous, and equilibrium phases and, whenever feasible, in a hepatocyte-specific phase.

Diffusion-weighted images were acquired using an EPI sequence with fat suppression (TR/TE, 2300/70 ms; matrix, 204×160; slice thickness, 8 mm; intersection gap, 1,6mm; field of view, 380 × 380 mm; ≈ 2 min acquisition time). The gradient factors (b-values) were 50 and 700 s/mm^2. For shortening echo train length, integrated parallel imaging techniques (iPAT) were used and, for respiratory triggering, PACE (prospective acquisition correction) was implemented. Data was acquired during the end-expiratory phase.

ADC maps were calculated automatically from all diffusion weightings on a voxel-by-voxel basis and three images were generated: b= 50 s/mm^2, b= 700 s/mm^2 and the correspondent ADC map.

Image Analysis

The Review of all MR images and previous exams was performed on a PACS workstation (SIENET Magic, v50, Siemens, 2004) and the review of the patient clinical history was performed using the internal database of our institution.

For lesion evaluation two procedures were performed: (a) for lesions > 20 mm, four values were obtained: 3 circular regions of interest (ROIs) with 1 cm^2 each were placed, randomly, inside the lesion, i.e. “ROI 1”, “ROI 2” and “ROI 3”, and 1 circular ROI was placed encompassing the most inside volume of lesion as possible, i.e. “ROI Total” (Fig. 1); (b) for lesions 10 mm to 20 mm, only one “ROI Total” was used. Due to software limitations, only circular ROIs were drawn. For comparing lesion ADC variations we used the ADC values of the ROI described before as “ROI Total”. When the lesion was not well visualized on the ADC map, the T2-weighted image, the contrast enhanced T1-weighted images and the b50 images served as a roadmap for accurate ROI placement.

For parenchymal evaluation, circular ROIs with a standard size of 1 cm^2 were placed, according to Couinaud’s segmentation, in four locations of the liver, away from vascular structures: segment II, anteriorly; segment IVb, centrally; segment VI, posteriorly and segment VIII, centrally.

Statistical Analysis

Statistical analysis was performed with SPSS software (version 18, SPSS). The Kruskal-Wallis test, with multiple comparisons by the Mann-Whitney test, was used to

calculate the significance of differences in the ADC values of different FHL, liver parenchyma and the differences between benign and malign lesions. The Friedman test was used to compare the four different regions of the liver. Optimal ADC threshold values for lesion discrimination were determined by means of receiver operating characteristic (ROC) curve analysis, and corresponding sensitivities and specificities were calculated. To assess the influence of ROI size and position we used the Wilcoxon test, comparing each one of the 1 cm^2 ROIs with the ROI comprising the total of the lesion, and the Spearman's correlation coefficient to compare each one of the 1 cm^2 ROIs with the mean value of the three. Bonferroni correction was used for multiple pair-wise comparisons and a p value of <0.05 was considered significant for all analyses.

RESULTS

Evaluation of hepatic parenchyma

For normal liver parenchyma a mean ADC value of 1.45 $\times 10^{-3}$ mm^2/s was obtained. Livers with cirrhosis or steatosis were found to have significantly lower mean ADC values (1.28 $\times 10^{-3} mm^2/s$ and 1.25 $\times 10^{-3} mm^2/s$, respectively) compared with normal liver parenchyma ($p<0.001$), but no significant difference was found between cirrhosis and steatosis. Mean ADC values obtained from normal, cirrhotic and steatotic livers are summarized in table 1.

When comparing mean ADC values of four different locations in the liver (Fig. 2), we found similarities between segments VI and VIII ($p\approx1$). However, segment VI revealed slightly lower ADC values and segment II showed higher ADC values compared to all other segments ($p<0.001$). The mean ADC values of the right lobe of the liver, 1.26 $\times 10^{-3} mm^2/s$, were significantly lower than ADC values of left lobe, 1.54 $\times 10^{-3} mm^2/s$ ($p<0.001$).

Evaluation of focal hepatic lesions

No markedly heterogeneous lesions were found in our study population. The mean ADCs of the several focal lesions (Table 2) was as follows ($\times 10^{-3} mm^2/s$): hepatocellular carcinoma (HCC), 1.18±0.17; metastases, 1.16±0.25; hepatocellular adenoma, 1.30±0.39; focal nodular hyperplasia (FNH), 1.64±0.41; hemangioma, 1.89±0.33; cyst, 2.77±0.58.

There was no significant difference between ADC values of HCCs, metastases and hepatocellular adenomas ($p=1$). ADC values of FNHs showed no significant difference from HCC ($p=0.281$), metastases ($p=0.200$), adenomas ($p=1$) or hemangiomas ($p=0.440$). HCCs

and metastatic lesions presented significantly lower ADC values compared to hemangiomas and cysts ($p<0.001$) and ADC values of cysts were significantly higher when compared to all other lesions (adenomas and FNHs, $p<0.05$ and HCCs and metastasis, $p<0.001$) except hemangiomas ($p=0.178$). The box-plots of the ADC values of HCCs, metastases, hepatocellular adenomas, FNHs, hemangiomas and cysts are depicted in Fig. 3. ADC values of metastases overlapped strongly with ADC values of HCCs, hepatocellular adenomas and FNH, and to some extent with ADC values of hemangiomas. ADC values of hemangiomas also strongly overlapped with FNH and partially overlapped with those of hepatocellular adenomas and cysts.

Mean ADC value of the 58 benign lesions was $2.02 \times 10^{-3} mm^2/s$, while mean ADC value of the 32 malignant lesions was $1.17 \times 10^{-3} mm^2/s$. The mean ADC values of malignant lesions were significantly lower than those of benign lesions, ($p<0.001$) (Fig. 4). The ROC curve analysis (Fig. 5), demonstrated that ADC measurements accurately differentiated between benign and malignant liver lesions with an area under the curve of 0,939 (95% CI: 0.888 to 0.991), a sensitivity of 89.7% and a specificity of 90.6%, using a cutoff ADC value of 1.43×10^{-3} mm^2/s.

Evaluation of region of interest

When comparing the three used methods of ROI placement (Fig. 6), no significant difference was found ($p=0,964$) between each ROI of 1 cm^2 ("ROI1, "ROI2" and "ROI3"), the average value of those three ROIs and the ROI encompassing the full inside of the lesion ("ROI Total"), in the overall lesions. When comparing the same sampling methods separately for each lesion type, also no significant difference was found (HCCs, $p=0.463$; metastases, $p=0.973$; adenomas, $p=0.525$; FNHs, $p=0.861$; hemangiomas, $p=0.481$ and cysts, $p=0.525$).

DISCUSSION

In accordance to previous publications (3,6,12,13,15,20,22-24), our findings demonstrated, with different degrees of overlap, lower ADC values in cirrhotic and steatotic livers when compared with normal hepatic parenchyma. Despite our overall measurements of normal and cirrhotic parenchyma being higher than those described by Bruegel et al (15) (average ADC value of normal parenchyma, $1.45\times10^{-3}mm^2/s$ versus $1.24\times10^{-3}mm^2/s$ and cirrhotic parenchyma, $1.28\times10^{-3}mm^2/s$ versus $1.04\times10^{-3}mm^2/s$), Taouli and coworkers (12), reported ADC values for normal parenchyma (with b= 0 and 400 sec/mm^2) which are closer to ours. Moreover, they also reported similar values, although slightly higher, to those described by Muller et al (6) and Kim et al (13). Girometti et al (24) also reported lower ADCs in cirrhotic livers compared with those of healthy controls , Qayyum et al (3) observed that liver ADC was significantly lower in 63 patients with nonalcoholic fatty liver disease than in healthy volunteers and Lewin et al (23) suspected a possible influence of steatosis on ADC values while analyzing inflammation scores.

A suggested explanation is that chronic fatty liver disease can lead to hepatic injury, fibrosis and cirrhosis, probably related to oxidative stress caused by intracellular accumulation of triglycerides and fatty acids (29). The cirrhotic condition reveals as restricted diffusion (3,6), which is probably explained by a multifactorial mechanism related to collagen deposition (which is proton poor) and decreased blood flow, as shown in some dynamic contrast-enhanced MRI studies (1-3,29,30). Although DWI can help differentiate between normal and pathological parenchyma, the strong overlap between ADC values in cirrhosis and steatosis, as stated before, doesn't allow the use of DWI as a stand-alone procedure for the differentiation between these two conditions.

When comparing the ADC values of different hepatic segments, our findings are concordant to the study by Bruegel et al (15). By evaluating the same hepatic areas as us (Table 1), they also reported that liver parenchyma in segment II displayed higher ADC values than any other segment. Kandpal et al (11) also found significantly higher mean ADC values in the left lobe of the liver using RT and breath-hold DWI. They placed a circular ROI on parenchyma areas adjacent to the lesions, avoiding artifacts and vascular areas, and reported average right lobe ADCs of 1.39 ± 0.28 ($\times 10^{-3}$ mm^2/s) and left lobe ADCs of 1.66 ± 0.41 ($\times 10^{-3}$ mm^2/s), with the RT technique.

The fact that segment II has higher ADC values can be explained by the increase exposure of this segment to cardiac motion artifacts (31). Such artifacts are more pronounced at higher b-values and when breath-hold imaging is used, and they can result in artificially high ADC values over the left hepatic lobe (17). Mürtz et al. (31) tested a pulse triggered technique in different abdominal organs and observed that ADCs acquired without pulse triggering were artificially increased by motion influences, particularly in regions close to the hearth or diaphragm. In fact, the use of cardiac triggering is a possible solution to the problem but, unlike respiratory triggering, it significantly increases image acquisition time (11). It has also been suggested that multiple averages can increase the probability of data acquisition in the diastolic phase and thus minimize cardiac motion-related signal loss but at the cost of a longer acquisition time (17).

ADC values of different FHL from different reports are shown in table 3. We chose to compare studies using RT sequences in order to minimize differences, since it is reported that ADC measurements obtained from the RT technique cannot be directly compared to those obtained with other techniques (i.e., free-breathing or breath-hold) (32). Plus, RT DW-EPI was found to show overall better image quality and higher lesion-to-liver contrast ratio and

was superior in ADC quantification and signal-to-noise ratio when compared with free-breathing and breath-hold techniques (10,11).

Low ADC values mean restricted diffusion (highly cellular tissues), while high ADC values signify free diffusion (tissues with low cellularity)(1-3). Unsurprisingly, cysts exhibited the highest ADC values because of their fluid content (Fig. 7), whereas highly cellular tumoral tissues like HCCs and metastases showed the lowest ADC values. Since HCC ADCs strongly overlapped with those of cirrhotic parenchyma, these lesions may be difficult to differentiate from surrounding cirrhosis or dysplastic nodules. Still, Zech et al (33) reported higher sensitivity for DWI compared to conventional MRI in detecting HCCs in cirrhotic liver. On the other hand, benign lesions had an overall intermediate ADC which overlaps with those of normal liver parenchyma but, despite this, they were significantly different when compared with other solid hepatic lesions, particularly HCCs.

In conformity with former studies, no overlap was found between the ADCs of cysts and solid lesions and all simple cysts had higher ADC values than the mean ADC value of hemangiomas. Although metastases showed significantly lower mean ADC values than benign lesions, there was a strong overlap with benign hepatocellular FHL and partial overlap with hemangiomas. The overlap with hemangiomas is of particular clinical interest since necrotic metastases may be strongly hyperintense (17,26,34), and hemangiomas may hyalinize and show decreased signal intensity on T2-weighted images (35) or may demonstrate atypical contrast enhancement patterns, similar to those of hypervascular metastases (15).

Differentiating benign from malignant hepatic lesions is a frequent diagnostic problem at MR imaging (12). Previous publications reported the ability of DWI in differentiating malignant from benign lesions by measuring ADC (7,10-16,20,21). All studies reported lower ADC values in malignant lesions when compared with benign ones, with different degrees of

overlap (table 3). However, different b-values were used and different lesion sizes were considered, impairing the comparison of results. We achieved a cutoff ADC value of 1.43 $\times 10^{-3}$ mm^2/s for differentiation, close to that proposed by Gourtsoyianni et al (20) and Holzapfel et al (21). We believe that our sensitivity and specificity values are slightly lower than those of Gourtsoyianni et al (20) and Taouli et al (10) mainly because these authors analyzed a lower number of lesions with intermediate ADC (i.e. hepatocellular adenomas and FNHs): the latter study considered only one FNH while the former evaluated none. It is known that FNH and adenomas, being hypercellular lesions, are expected to present low ADC values (10,20) and so, we believe that the potential of ADC for lesion characterization was overestimated in both their studies due to the small number of benign solid lesions included.

All studies in literature show large discrepancies regarding ADC values in the abdomen. For example, compiled data until 2008 (15) reported mean ADCs for normal hepatic parenchyma ranging from 0.69 to 2.28 $\times 10^{-3} mm^2/s$. Those equivocal results can be due to differences in MR scanners and to the lack of a standardized DWI protocol regarding the optimum imaging acquisition parameters (11,16).

Besides those technical limitations, it is documented that the different size and type of lesions considered (15) and the different characteristics of the chosen ROIs had substantial influence on the resulting ADCs. ROIs are drawn on the basis of personal visual ability (28) and the different areas where the ROIs are placed are important. A more centrally placed ROI (i.e., located further from the receiver coils) is exposed to more noise contamination (15) and it has been suggested that low SNR can lead to underestimated ADC values (36). Recent publications (28,37) reported that it remains unclear whether ADC evaluation should include the entire lesion volume or a representative lesion section, and whether the representative lesion section is sufficient to fully characterize it.

From our data we conclude that no difference was found between using one ROI of 1 cm^2 or using a ROI that encompasses all lesion volume. However, in our study population no markedly heterogeneous lesions were found. It has been reported that metastases with necrotic areas can show areas with higher ADC values (34) and hyalinized hemangiomas can show areas with lower ADC value (35), so it is easily understandable that some unusual findings are lacking in our data. Although our results cannot be generalized, we suggest that, in homogenous lesions, a circular supra-centimetric ROI can provide accurate ADC measurements. However, as stated before, ROI placement is debatable, not objective and subject to considerable variation. As an example, both Colagrande et al (28) and Goh et al (37) reported the influence of ROI size and position (in the ADC value and in the estimated tumor perfusion, respectively). The first author studied normal hepatic parenchyma with DWI, while the second analyzed colorectal carcinoma using computed tomography.

Our study had several limitations. The first major limitation was the low number of lesions and the lack of correlative histopathological data in most cases. More intermediate lesions, i.e. adenomas and FNHs, could theoretically have lowered our accuracy in characterizing FHL since those lesions show intermediate ADC value that can overlap with normal liver parenchyma and malignant lesions. Future studies with a larger number of patients are needed and those should understand that very high ADC values seen in cysts (commonly found) can falsely increase DWI's ability to differentiate between benign and malignant lesions. Second, we have to consider two potential sources of selection bias. The fact that we excluded infra-centimetric lesions that usually present slightly lower ADC values than other lesions (15,21), and the fact that, in patients with multiple FHL, only the largest lesions were analyzed. Third, despite the fact that most of the lesions are round-shaped, our study should have included the freehand tool for drawing a ROI since it is currently used in

the clinical setting. Forth, as stated before, no markedly heterogeneous legions were present in our study population.

In conclusion, quantitative ADC values of hepatic parenchyma and focal hepatic lesions can yield information about parenchymal and lesional characterization, in this latter case useful for the differential diagnosis between malignant and benign lesions. There is a significant diffusion restriction in cirrhosis and steatosis, and significantly lower ADC values in malignant lesions when compared with benign ones. However, as there is overlap between different types of lesions, DWI should not be considered as a stand-alone procedure, especially in the assessment of solid benign lesions that may exhibit restricted diffusion mimicking malignant lesions. A lesion ROI above 1 cm^2 can provide accurate ADC values measured in supra-centimetric homogenous lesions. Other lesions should be studied and future cutoffs for lesion characterization should be obtained, using a standardized DWI protocol to overcome differences between studies.

ACKNOWLEDGMENTS

The authors thank Dr. Bárbara Oliveiros (Instituto de Biofísica e Biomatemática, IBILI – FMUC, Portugal), Dr. João Casalta (Instituto de Biofísica e Biomatemática, IBILI – FMUC, Portugal) and Dr. Miguel Seco (Clínica Universitária de Radiologia, Hospitais da Universidade de Coimbra, Portugal) for the support in the production of this work.

REFERENCES

1. Taouli B, Koh D-M. Diffusion-weighted MR imaging of the liver. Radiology. 2010 Jan;254(1):47-66.

2. Kele PG, van der Jagt EJ. Diffusion weighted imaging in the liver. World J. Gastroenterol. 2010 Abr 7;16(13):1567-1576.

3. Qayyum A. Diffusion-weighted imaging in the abdomen and pelvis: concepts and applications. Radiographics. 2009 Out;29(6):1797-1810.

4. Stejskal EO, Tanner JE. Spin Diffusion Measurements: Spin Echoes in the Presence of a Time-Dependent Field Gradient. J. Chem. Phys. 1965;42(1):288.

5. Thoeny HC, De Keyzer F. Extracranial applications of diffusion-weighted magnetic resonance imaging. Eur Radiol. 2007 Jun;17(6):1385-1393.

6. Müller MF, Prasad P, Siewert B, Nissenbaum MA, Raptopoulos V, Edelman RR. Abdominal diffusion mapping with use of a whole-body echo-planar system. Radiology. 1994 Fev;190(2):475-478.

7. Demir OI, Obuz F, Sağol O, Dicle O. Contribution of diffusion-weighted MRI to the differential diagnosis of hepatic masses. Diagn Interv Radiol. 2007 Jun;13(2):81-86.

8. Koh D-M, Collins DJ. Diffusion-weighted MRI in the body: applications and challenges in oncology. AJR Am J Roentgenol. 2007 Jun;188(6):1622-1635.

9. Koh D-M, Takahara T, Imai Y, Collins DJ. Practical aspects of assessing tumors using clinical diffusion-weighted imaging in the body. Magn Reson Med Sci. 2007;6(4):211-224.

10. Taouli B, Sandberg A, Stemmer A, Parikh T, Wong S, Xu J, et al. Diffusion-weighted imaging of the liver: comparison of navigator triggered and breathhold acquisitions. J Magn Reson Imaging. 2009 Set;30(3):561-568.

11. Kandpal H, Sharma R, Madhusudhan KS, Kapoor KS. Respiratory-triggered versus breath-hold diffusion-weighted MRI of liver lesions: comparison of image quality and apparent diffusion coefficient values. AJR Am J Roentgenol. 2009 Abr;192(4):915-922.

12. Taouli B, Vilgrain V, Dumont E, Daire J-L, Fan B, Menu Y. Evaluation of liver diffusion isotropy and characterization of focal hepatic lesions with two single-shot echo-planar MR imaging sequences: prospective study in 66 patients. Radiology. 2003 Jan;226(1):71-78.

13. Kim T, Murakami T, Takahashi S, Hori M, Tsuda K, Nakamura H. Diffusion-weighted single-shot echoplanar MR imaging for liver disease. AJR Am J Roentgenol. 1999 Ago;173(2):393-398.

14. Parikh T, Drew SJ, Lee VS, Wong S, Hecht EM, Babb JS, et al. Focal liver lesion detection and characterization with diffusion-weighted MR imaging: comparison with standard breath-hold T2-weighted imaging. Radiology. 2008 Mar;246(3):812-822.

15. Bruegel M, Holzapfel K, Gaa J, Woertler K, Waldt S, Kiefer B, et al. Characterization of focal liver lesions by ADC measurements using a respiratory triggered diffusion-weighted single-shot echo-planar MR imaging technique. Eur Radiol. 2008 Mar;18(3):477-485.

16. Goshima S, Kanematsu M, Kondo H, Yokoyama R, Kajita K, Tsuge Y, et al. Diffusion-weighted imaging of the liver: optimizing b value for the detection and characterization of benign and malignant hepatic lesions. J Magn Reson Imaging. 2008 Set;28(3):691-697.

17. Nasu K, Kuroki Y, Nawano S, Kuroki S, Tsukamoto T, Yamamoto S, et al. Hepatic metastases: diffusion-weighted sensitivity-encoding versus SPIO-enhanced MR imaging. Radiology. 2006 Abr;239(1):122-130.

18. Coenegrachts K, Delanote J, Ter Beek L, Haspeslagh M, Bipat S, Stoker J, et al. Improved focal liver lesion detection: comparison of single-shot diffusion-weighted echoplanar and single-shot T2 weighted turbo spin echo techniques. Br J Radiol. 2007 Jul;80(955):524-531.

19. Sandrasegaran K, Akisik FM, Lin C, Tahir B, Rajan J, Aisen AM. The value of diffusion-weighted imaging in characterizing focal liver masses. Acad Radiol. 2009 Out;16(10):1208-1214.

20. Gourtsoyianni S, Papanikolaou N, Yarmenitis S, Maris T, Karantanas A, Gourtsoyiannis N. Respiratory gated diffusion-weighted imaging of the liver: value of apparent diffusion coefficient measurements in the differentiation between most commonly encountered benign and malignant focal liver lesions. Eur Radiol. 2008 Mar;18(3):486-492.

21. Holzapfel K, Bruegel M, Eiber M, Ganter C, Schuster T, Heinrich P, et al. Characterization of small (≤10 mm) focal liver lesions: value of respiratory-triggered echo-planar diffusion-weighted MR imaging. Eur J Radiol. 2010 Out;76(1):89-95.

22. Taouli B, Tolia AJ, Losada M, Babb JS, Chan ES, Bannan MA, et al. Diffusion-weighted MRI for quantification of liver fibrosis: preliminary experience. AJR Am J Roentgenol. 2007 Out;189(4):799-806.

23. Lewin M, Poujol-Robert A, Boëlle P-Y, Wendum D, Lasnier E, Viallon M, et al. Diffusion-weighted magnetic resonance imaging for the assessment of fibrosis in chronic hepatitis C. Hepatology. 2007 Set;46(3):658-665.

24. Girometti R, Furlan A, Esposito G, Bazzocchi M, Como G, Soldano F, et al. Relevance of b-values in evaluating liver fibrosis: a study in healthy and cirrhotic subjects using two single-shot spin-echo echo-planar diffusion-weighted sequences. J Magn Reson Imaging. 2008 Ago;28(2):411-419.

25. Feuerlein S, Pauls S, Juchems MS, Stuber T, Hoffmann MHK, Brambs H-J, et al. Pitfalls in abdominal diffusion-weighted imaging: how predictive is restricted water diffusion for malignancy. AJR Am J Roentgenol. 2009 Out;193(4):1070-1076.

26. Cui Y, Zhang X-P, Sun Y-S, Tang L, Shen L. Apparent diffusion coefficient: potential imaging biomarker for prediction and early detection of response to chemotherapy in hepatic

metastases. Radiology. 2008 Set;248(3):894-900.

27. Goshima S, Kanematsu M, Kondo H, Yokoyama R, Tsuge Y, Shiratori Y, et al. Evaluating local hepatocellular carcinoma recurrence post-transcatheter arterial chemoembolization: is diffusion-weighted MRI reliable as an indicator? J Magn Reson Imaging. 2008 Abr;27(4):834-839.

28. Colagrande S, Pasquinelli F, Mazzoni LN, Belli G, Virgili G. MR-diffusion weighted imaging of healthy liver parenchyma: repeatability and reproducibility of apparent diffusion coefficient measurement. J Magn Reson Imaging. 2010 Abr;31(4):912-920.

29. Taouli B, Ehman RL, Reeder SB. Advanced MRI methods for assessment of chronic liver disease. AJR Am J Roentgenol. 2009 Jul;193(1):14-27.

30. Hagiwara M, Rusinek H, Lee VS, Losada M, Bannan MA, Krinsky GA, et al. Advanced liver fibrosis: diagnosis with 3D whole-liver perfusion MR imaging--initial experience. Radiology. 2008 Mar;246(3):926-934.

31. Mürtz P, Flacke S, Träber F, van den Brink JS, Gieseke J, Schild HH. Abdomen: diffusion-weighted MR imaging with pulse-triggered single-shot sequences. Radiology. 2002 Jul;224(1):258-264.

32. Kwee TC, Takahara T, Koh D-M, Nievelstein RAJ, Luijten PR. Comparison and reproducibility of ADC measurements in breathhold, respiratory triggered, and free-breathing diffusion-weighted MR imaging of the liver. J Magn Reson Imaging. 2008 Nov;28(5):1141-1148.

33. Zech CJ, Reiser MF, Herrmann KA. Imaging of hepatocellular carcinoma by computed tomography and magnetic resonance imaging: state of the art. Dig Dis. 2009;27(2):114-124.

34. Koh DM, Scurr E, Collins DJ, Pirgon A, Kanber B, Karanjia N, et al. Colorectal hepatic metastases: quantitative measurements using single-shot echo-planar diffusion-weighted MR imaging. Eur Radiol. 2006 Set;16(9):1898-1905.

35. Vilgrain V, Boulos L, Vullierme MP, Denys A, Terris B, Menu Y. Imaging of atypical hemangiomas of the liver with pathologic correlation. Radiographics. 2000 Abr;20(2):379-397.

36. Dietrich O, Heiland S, Sartor K. Noise correction for the exact determination of apparent diffusion coefficients at low SNR. Magn Reson Med. 2001 Mar;45(3):448-453.

37. Goh V, Halligan S, Gharpuray A, Wellsted D, Sundin J, Bartram CI. Quantitative assessment of colorectal cancer tumor vascular parameters by using perfusion CT: influence of tumor region of interest. Radiology. 2008 Jun;247(3):726-732.

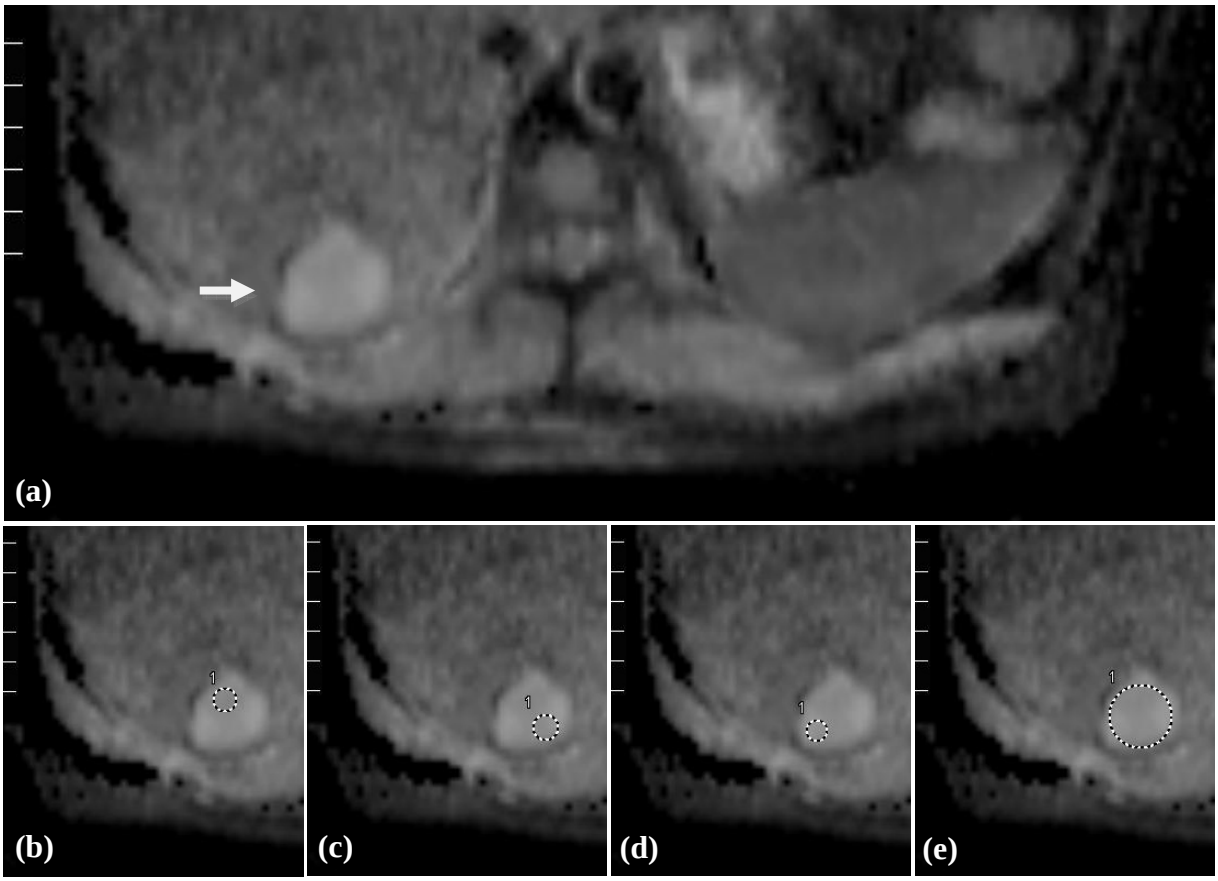

Fig. 1 Lesion sampling method. **(a)** ADC map of an 57-year-old women with an hemangioma (arrow), more intense than the surrounding parenchyma, measuring approximately 28 mm. **(b-d)** Three circular ROIs, measuring 1 cm^2 each, were placed randomly in different areas of the lesion ("ROI1", "ROI2" and "ROI3") and **(e)** one circular ROI, largest enough to encompass all area of the lesion, was placed inside the lesion ("ROI Total").

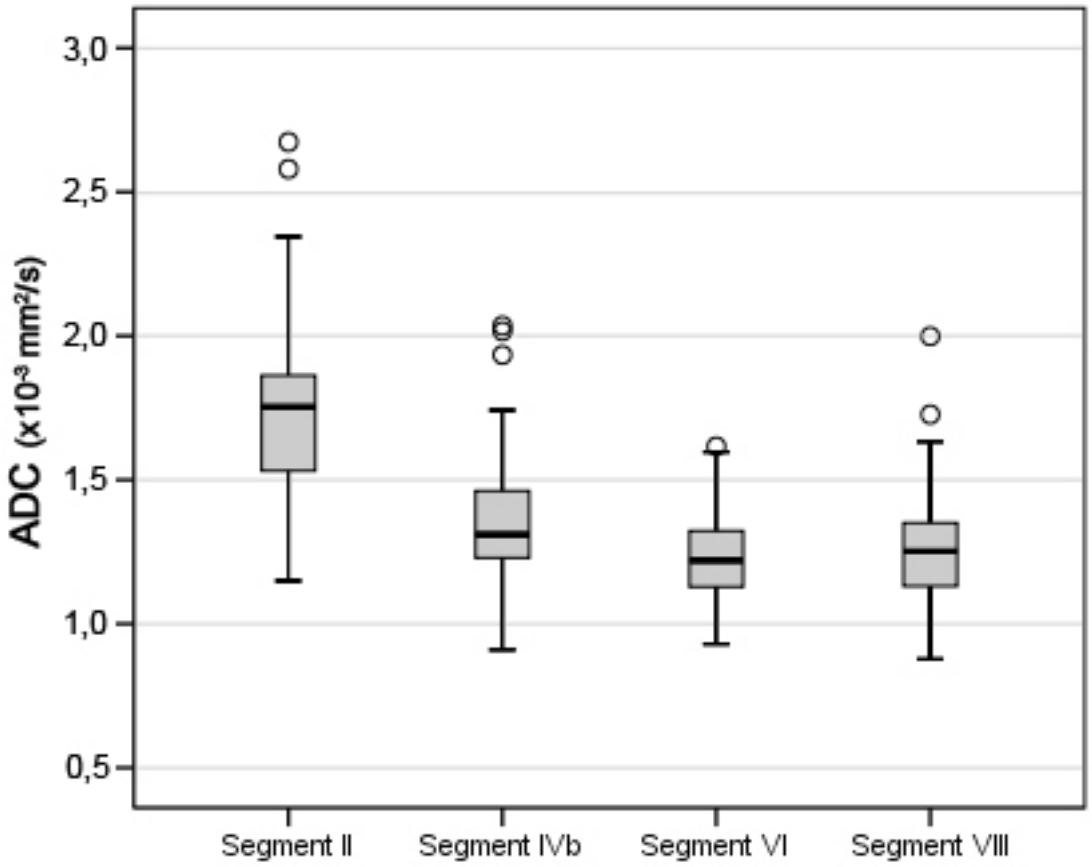

Fig. 2 Box plots showing parenchyma ADC values of four different segments of the liver. Boxes stretch from lower quartile to upper quartile (25th to 75th percentile); median is shown as a line across each bar; whiskers show sample minimum and maximum; O denotes outliners. ADC values of all segments overlap between each other. Segment II shows the highest ADC values and, globally, ADC values of the left lobe of the liver (segment II and segment IVb) are higher than those of the right lobe (segment VI and segment VIII).

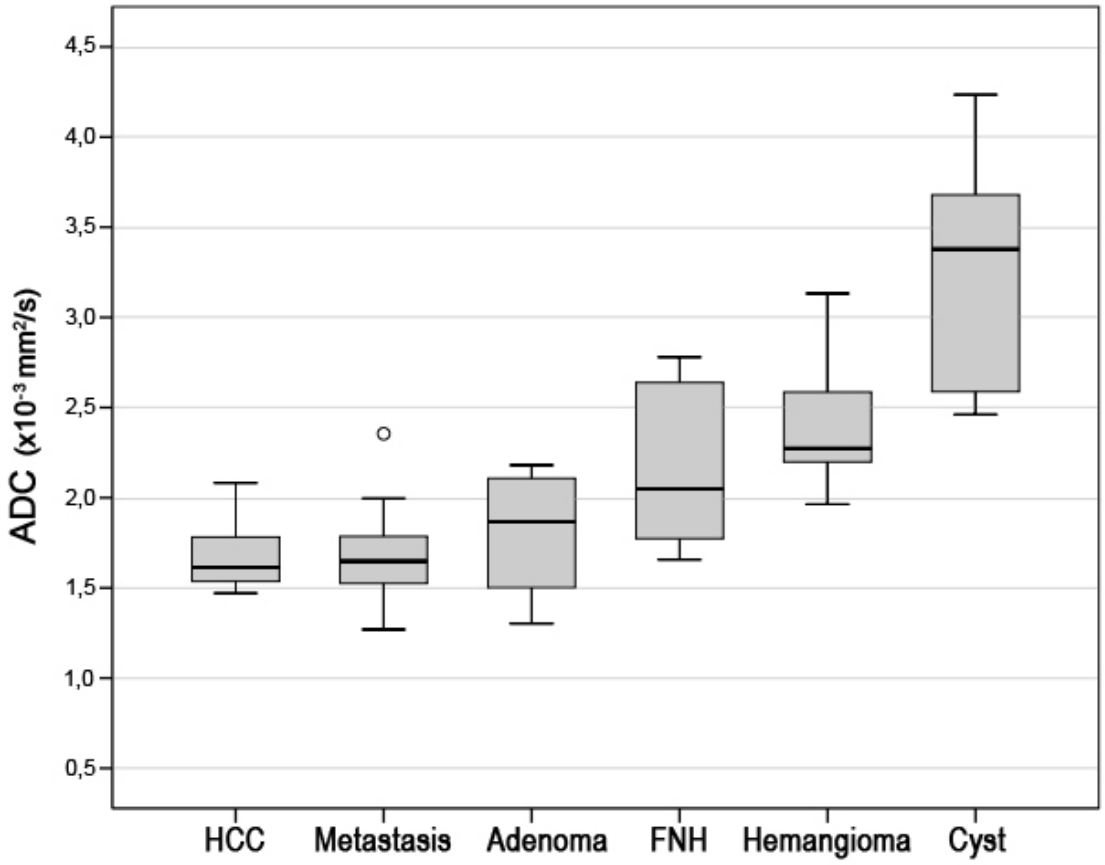

Fig. 3 Box plots showing the ADC values of 90 focal hepatic lesions. ADC values of HCCs overlapped with ADC values of metastases, adenomas, FNHs and hemangiomas. ADC values of hemangiomas also overlapped with ADC values of adenomas, FNHs and cysts.

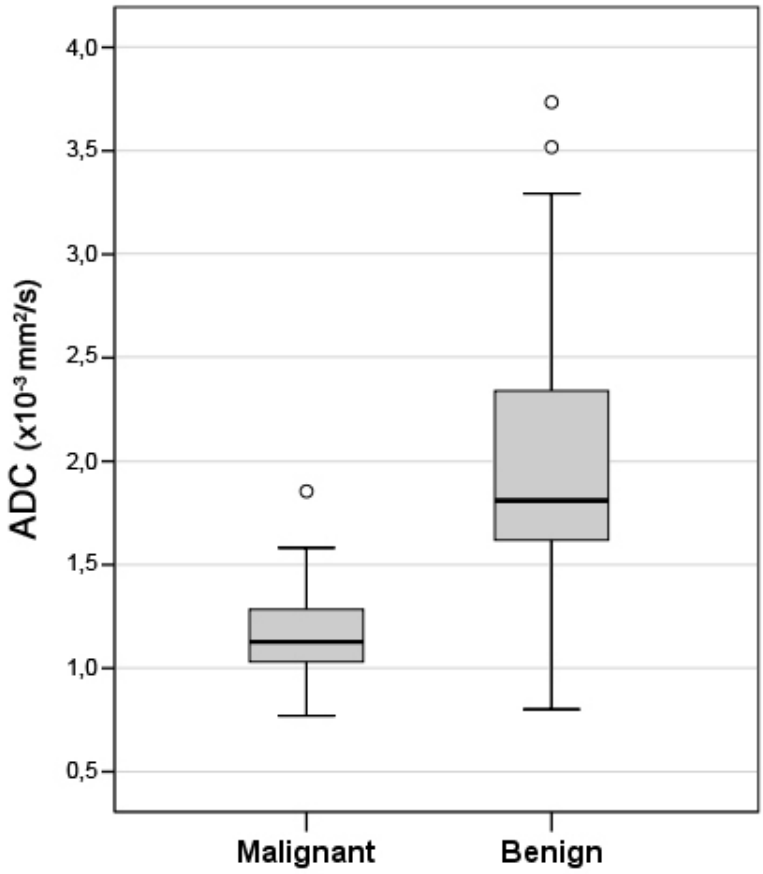

Fig. 4 Box plots showing ADC values calculated for 32 malignant and 58 benign focal hepatic lesions. Despite some overlap between malignant and benign focal hepatic lesions, differences in ADC values were statistically significant. Generally, benign lesions showed higher ADCs than malignant ones.

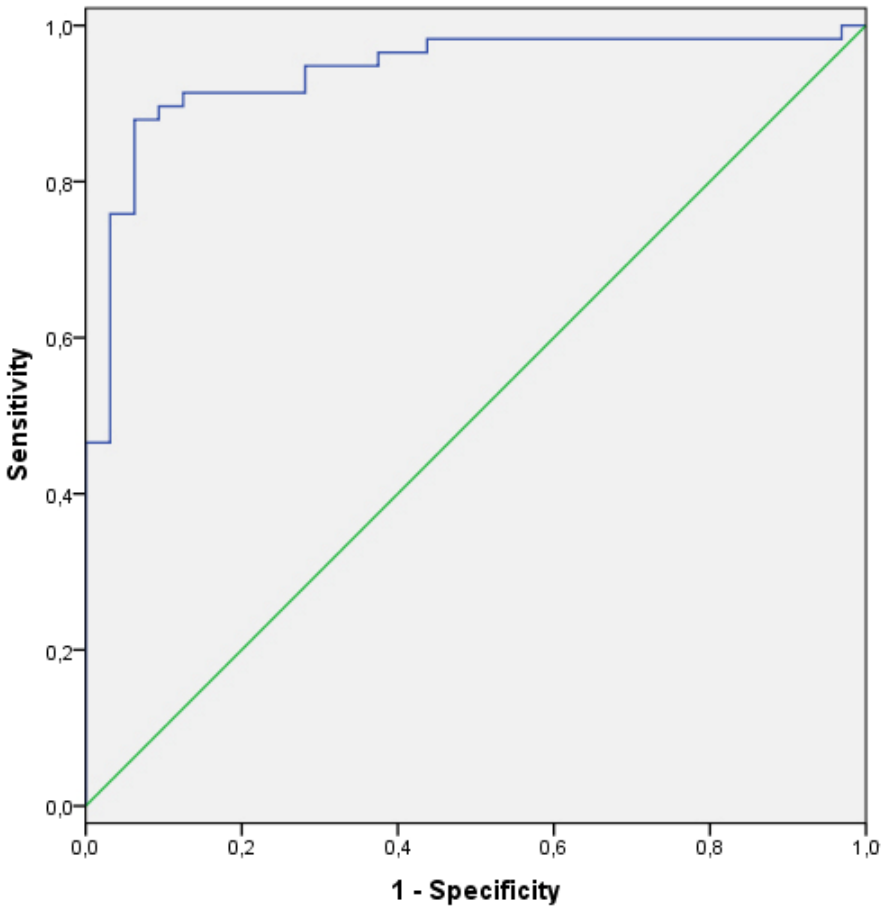

Fig. 5 Receiver operating characteristic (ROC) curve used for differentiation between malignant and benign lesions based on ADC values. The area under the curve (AUC) is 0.939. Using a threshold value of 1.43×10^{-3} mm^2/s it is possible to differentiate benign from malignant lesions with a sensitivity of 89.7% and a specificity of 90.6%.

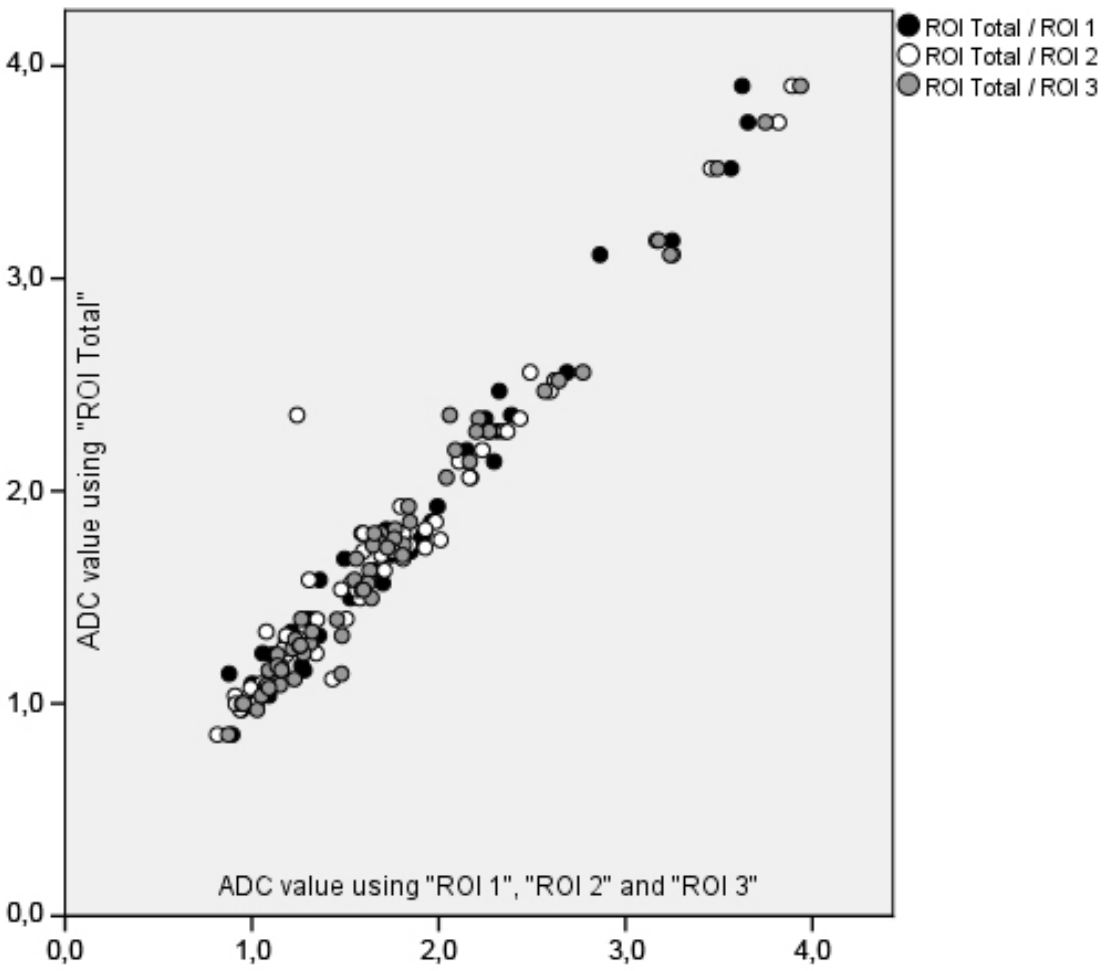

Fig. 6 Scatter plot showing correlation of ADC values obtained using standard circular 1 cm^2 regions of interest ("ROI 1", "ROI 2" and "ROI 3") and one circular ROI encompassing the largest possible area inside the lesion ("ROI Total"). There is a strong significant correlation between data. ADC values are expressed in $\times 10^{-3}$ mm^2/s.

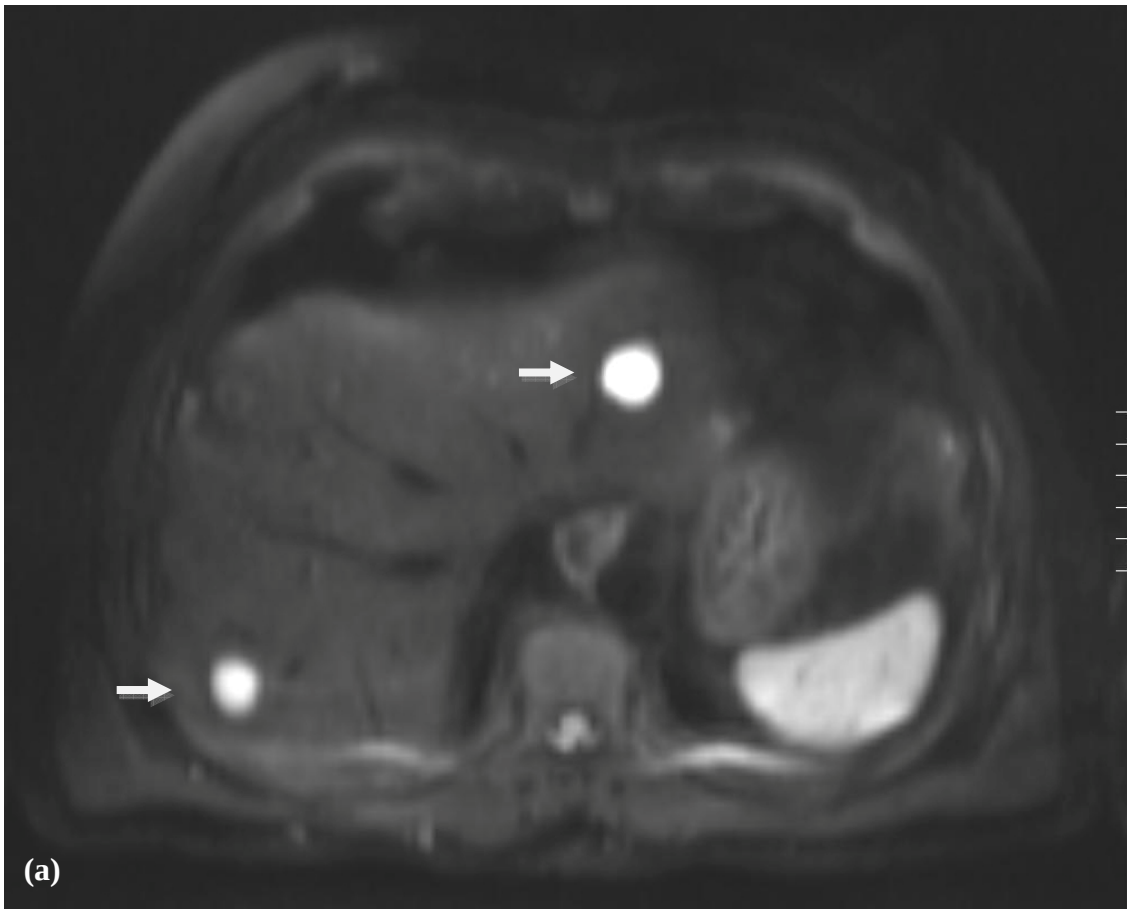
(a)

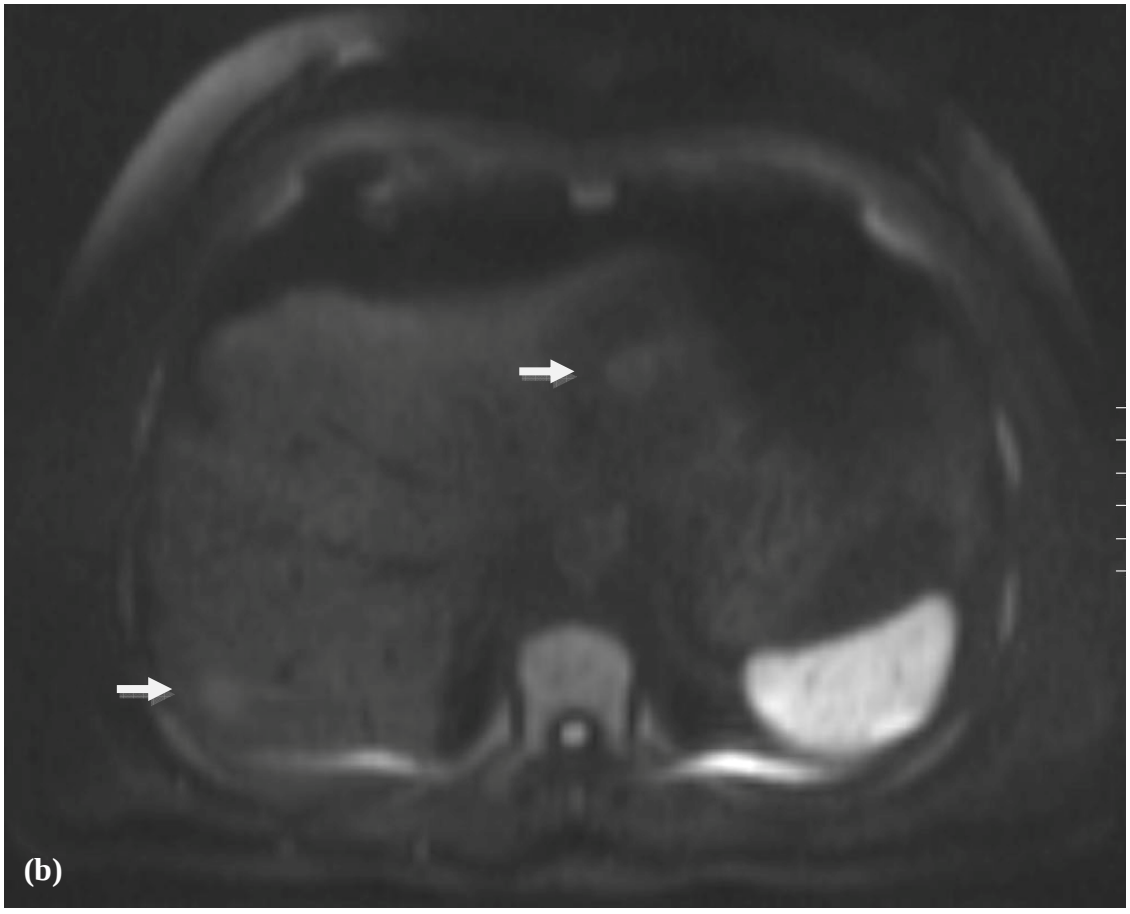
(b)

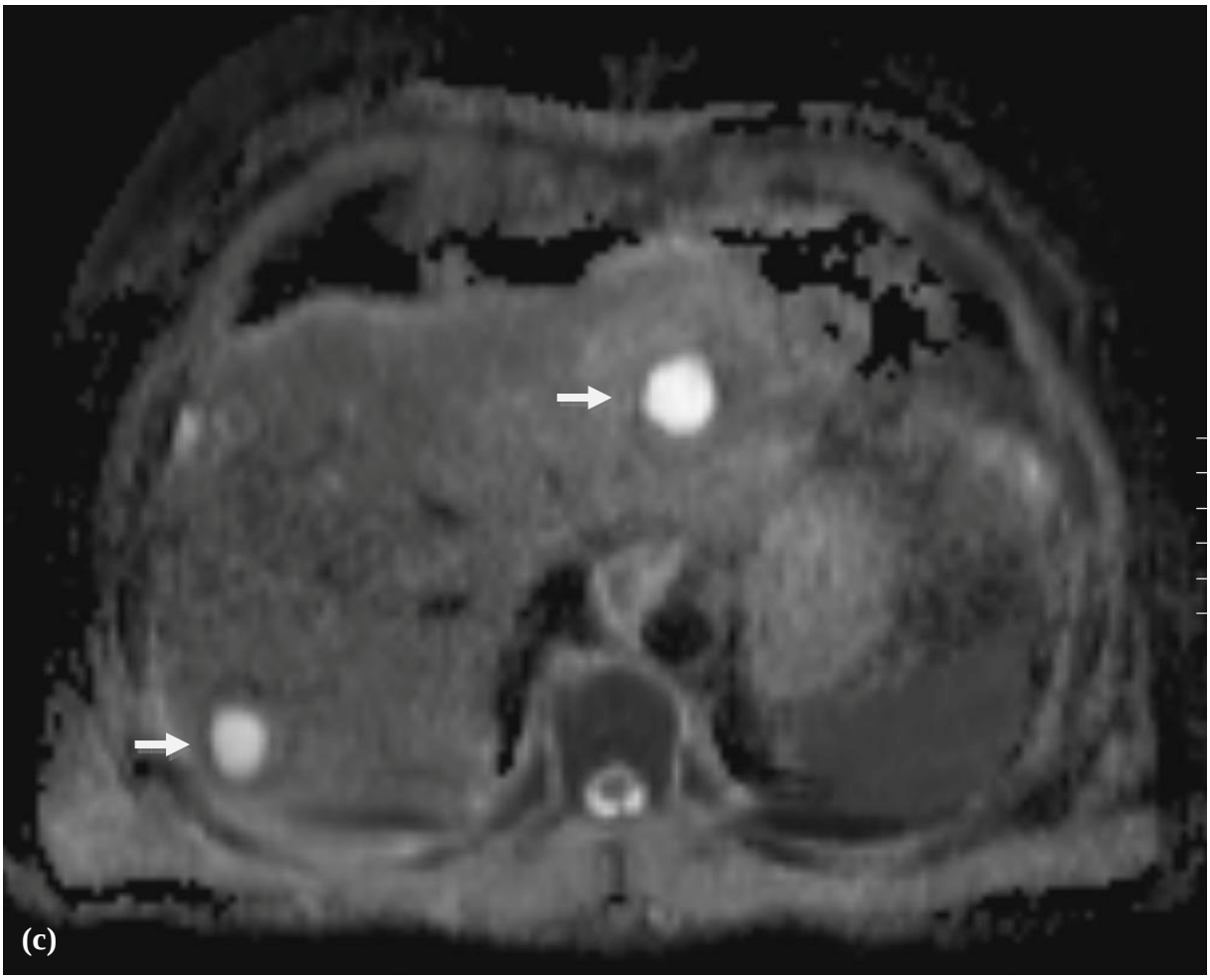

Fig. 7 66-year-old male patient with two hepatic cysts (arrows) confirmed by concordant imaging findings. **(a)** Diffusion-weighted image, using b-value= 50 s/mm^2, showing two markedly high intense lesions, in the right and left liver lobes. **(b)** At b-value= 700 s/mm^2 the lesion keeps high signal when compared with hepatic parenchyma, but decays in signal intensity when compared with b = 50 s/mm^2 (typical finding in low cellular lesions) which translates into an intense signal on the ADC map **(c)**, demonstrating unimpeded diffusion. Mean ADC of largest cyst, located in the left lobe, 3.11 $\times 10^{-3}$mm^2/s.

Table 1 ADC measured in four different liver segments

	ADC ($\times 10^{-3}$ mm^2/s) *
Normal Liver Parenchyma	
Segment II, anterior	1.83 ± 0.29
Segment IVb, central	1.39 ± 0.20
Segment VI, posterior	1.27 ± 0.15
Segment VIII, central	1.29 ± 0.18
Mean value of four segments	1.45 ± 0.16
Cirrhotic Liver Parenchyma	
Segment II, anterior	1.52 ± 0.21
Segment IVb, central	1.20 ± 0.14
Segment VI, posterior	1.18 ± 0.14
Segment VIII, central	1.21 ± 0.16
Mean value of four segments	1.28 ± 0.12
Steatotic Liver Parenchyma	
Segment II, anterior	1.57 ± 0.17
Segment IVb, central	1.25 ± 0.18
Segment VI, posterior	1.09 ± 0.08
Segment VIII, central	1.10 ± 0.15
Mean value of four segments	1.25 ± 0.13

* ADC is presented as mean value ± standard deviation.

Table 2 Size and apparent diffusion coefficient (ADC) of 90 focal hepatic lesions

	size (mm)		ADC (× 10^{-3} mm^2/s)	
	mean	**range**	**mean ± SD**	**95% CI**
HCC *(n=14)*	56,9	[15-135]	1,18 ± 0,17	1,08 - 1,28
Metastases *(n=18)*	39,8	[12-114]	1,16 ± 0,25	1,03 - 1,28
Adenomas *(n=4)*	28,2	[12-59]	1,30 ± 0,39	0,68 – 1,92
FNH *(n=10)*	39,0	[16-80]	1,65 ± 0,41	1,34 – 1,94
Hemangiomas *(n=30)*	31,0	[11-85]	1,89 ± 0,33	1,77 – 2,01
Cysts *(n=14)*	23,1	[10-51]	2,77 ± 0,58	2,44 – 3,11
Benign *(n=58)*			2,02 ± 0,61	1,86 – 2,18
Malignant *(n=32)*			1,17 ± 0,22	1,09 – 1,25

HCC, hepatocellular carcinoma; FNH, focal nodular hyperplasia; ADC, apparent diffusion coefficient; SD, standard deviation; CI, confidence interval

Table 3 Reported ADC values of Normal Liver Parenchyma and Focal Hepatic Lesions, and ADC Cutoffs with Sensitivity and Specificity for differentiation of malignant and benign lesions, in selected studies using diverse Respiratory Triggered DWI protocols.

	Bruegel et al (15)		**Gourtsoyianni et al** (20)		**Kandpal et al** (11)		**Holzapfel et al** (21)		**Taouli et al** (10)		**our study**	
b-values (s/mm^2)	50, 300, 600		0, 50, 500, 1000		0, 500		50, 300, 600		0, 50, 500		50, 700	
		n		*n*		*n*		*n*		*n*		*n*
Hepatic Parenchyma	1.24 ± 0.15	-	1.25 †	-	1.52 ‡	-	-	-	1.00 ± 0.27	-	1.45 ± 0.16	-
HCCs	1.05 ± 0.09	*11*	1.38	*2*	1.27 ± 0.42	*12*	1.12 ± 0.28	*17*	-	*7*	1.18 ± 0.17	*14*
Metastases	1.22 ± 0.31	*82*	0.99	*13*	1.13 ± 0.41	*38*	1.08 ± 0.32	*76*	-	*4*	1.16 ± 0.25	*18*
Adenomas	-	-	-	-	-	-	1.43 ± 0.22§	*9*	-	-	1.30 ± 0.39	*4*
FNH	1.40 ± 0.15	*4*	-	-	2.15 ± 0.18	*3*		*6*	-	*1*	1.65 ± 0.41	*10*
Hemangiomas	1.92 ± 0.34	*56*	1.90	*7*	2.36 ± 0.48	*11*	1.69 ± 0.34	*18*	-	*8*	1.89 ± 0.33	*30*
Cysts	3.02 ± 0.31	*51*	2.55	*15*	2.90 ± 0.51	*11*	2.61 ± 0.57	*71*	-	*9*	2.77 ± 0.58	*14*
Benign Lesions	-	-	2.55	*22*	-	-	2.36 ± 0.62	*104*	2.39 ± 0.44	*18*	2.02 ± 0.61	*32*
Malign Lesions	-	-	1.04	*15*	-	-	1.09 ± 0.30	*93*	1.16 ± 0.33	*11*	1.17 ± 0.22	*58*
Cutoff *	**1.63**		**1.47**				**1.41**		**1.50**		**1.43**	
Sensitivity (%)	90		100				90.8		100		89.7	
Specificity (%)	86		100				89.9		100		90.6	

Values are presented as ADC ± Standard Deviation ($\times 10^{-3}$ mm^2/s). Bruegel et al analyzed 204 lesions, 77 of which have less than 10 mm (38%) and reported that 88% of lesions could be correctly characterize with an ADC threshold of 1.63×10^{-3} mm^2/s. Gourtsoyianni et al and Kandpal et al didn't inform about the minimum size of lesions considered. Holzapfel et al only studied lesions ≤ 10 mm. Taouli et al considered lesions ranging from 7 mm to 90 mm. ADC, apparent diffusion coefficient; SD, standard deviation; n, number of occurrences; FNH, focal nodular hyperplasia; HCC, hepatocellular carcinoma.

* ADC cutoff for diagnosis of malignant hepatic lesions: Lesions with ADC below the proposed cutoff value are considered malignant, while those with ADC above are considered benign.

† This ADC value is referent only to 13 patients without FHL. Gourtsoyianni et al found no significant difference between the hepatic parenchyma of the ones with FHLs and the ones without FHLs.

‡ This ADC value was not presented in Kandpal et al study. It was calculated by us as an average of the right and left hepatic lobes, for comparative purpose.

§ In Holzapfel et al article, the ADC values for FNH and adenomas are presented together.